◆ Human Brain Mapping 36:2691–2702 (2015) ◆

Age and Sex Effects on Corpus Callosum Morphology Across the Lifespan

Daniel M. Prendergast,[1,2,3]* Babak Ardekani,[4] Toshikazu Ikuta,[5] Majnu John,[1,2,6] Bart Peters,[1,2] Pamela DeRosse,[1,2] Robin Wellington,[3] Anil K. Malhotra,[1,2,7,8] and Philip R. Szeszko[1,2,7,8]

[1]Center for Psychiatric Neuroscience, The Feinstein Institute for Medical Research, North Shore-LIJ Health System, Manhasset, New York
[2]Department of Psychiatry Research, The Zucker Hillside Hospital, North Shore-LIJ Health System, Glen Oaks, New York
[3]Department of Psychology, St. John's University, Queens, New York
[4]Center for Advanced Brain Imaging, Nathan S. Kline Institute for Psychiatric Research, Orangeburg, New York
[5]Department of Communication Sciences and Disorders, School of Applied Sciences, University of Mississippi, University, Mississippi
[6]Department of Mathematics, Hofstra University, Hempstead, New York
[7]Department of Psychiatry, Hofstra North Shore – LIJ School of Medicine, Hempstead, New York
[8]Department of Molecular Medicine, Hofstra North Shore – LIJ School of Medicine, Hempstead, New York

Abstract: The corpus callosum (CC) is the largest interhemispheric white matter tract in the human brain, and is characterized by pronounced differences in morphology among individuals. There are limited data, however, regarding typical development, sex differences, and the neuropsychological correlates of individual differences within CC subregions. Magnetic resonance (MR) imaging exams were collected in a large cohort ($N = 305$) of healthy individuals (ages 8–68). We used a highly reliable program to automatically identify the midsagittal plane and obtain CC subregion measures according to approaches described by Witelson [1989]: Brain 112:799–835 and Hampel et al. [1998]: Arch Neurol 55:193–198 and a measure of whole CC shape (i.e., circularity). CC measurement parameters, including area, perimeter, length, circularity, and CC subregion area values were generally characterized by inverted U-shaped curves across the observed age range. Peak values for CC subregions were observed between ages 32 and 45, and descriptive linear correlations were consistent with sharper area changes in development. We also observed differing age-associated changes across the lifespan between males and females in the CC subregion corresponding to the genu (Witelson's subregion 2), as well as CC circularity. Mediation analysis using path modeling indicated that genu area mediated

Contract grant sponsors: NARSAD (PRS) and the National Institute of Mental Health; Contract grant number: MH76995 (PRS); Contract grant sponsor: the NSLIJ Research Institute General Clinical Research Center and the National Institute of Mental Health; Contract grant number: M01 RR18535; Contract grant sponsor: an Advanced Center for Intervention and Services Research; Contract grant number: MH74543; Contract grant sponsor: Center for Intervention Development and Applied Research; Contract grant number: MH80173

*Correspondence to: Daniel Prendergast, Zucker Hillside Hospital, North Shore-LIJ Health System, Psychiatry Research, 75-59 263rd Street, Glen Oaks, NY 11004.
E-mail: dmprendergast@gmail.com

Received for publication 22 November 2014; Revised 16 February 2015; Accepted 13 March 2015.

DOI: 10.1002/hbm.22800
Published online 2 April 2015 in Wiley Online Library (wileyonlinelibrary.com).

the relationship between age and processing speed for females, and the relationship between age and visual learning and executive functioning for males. Taken together, our findings implicate sex differences in CC morphology across the lifespan that are localized to the genu, which appear to mediate neuropsychological functions. *Hum Brain Mapp 36:2691–2702, 2015.*

Key words: corpus callosum; sex differences; lifespan; neuropsychological functioning

INTRODUCTION

The corpus callosum (CC) is the largest white matter (WM) tract and interhemispheric commissure in the human brain [Huang et al., 2005]. The midsagittal segment of the CC is topographically organized such that its connective fibers run perpendicular to the cerebral falx and generally correspond to homologous regions of contralateral cortex [Chao et al., 2009; Hasan et al., 2009; Hofer and Frahm, 2006; Lebel et al., 2010]. In the typically developing human brain, roughly 250–300 million axons traverse the midsagittal CC [Aboitiz et al., 1992] with the number of fibers comprising the CC believed to be largely fixed at birth [Luders et al., 2010]. The CC is structurally and functionally heterogeneous, and across different subregions cell axons vary substantially in number, density, diameter [Aboitiz et al., 1992; van der Knaap and van der Ham, 2011], and diffusion properties [Lebel et al., 2010]. Moreover, midsagittal CC demonstrates substantial interindividual variability in local morphology including area, perimeter, length, thickness, and shape among healthy individuals [Bruner et al., 2012; Suganthy et al., 2003]. Despite variability in whole, subregion and shape CC parameters, neuroimaging studies investigating these properties in large cohorts of healthy individuals across a wide age range are lacking.

There remains considerable controversy regarding the effects of age and sex on CC morphology [Ardekani et al., 2012; Bruner et al., 2012; Luders, et al., 2010], following early postmortem work reporting a more bulbous splenium in females compared to males, as well as larger midsagittal CC area in males [DeLacoste-Utamsing and Holloway, 1982; Holloway and DeLacoste, 1986]. Following over a decade of research, an early meta-analysis reported absolute CC area is larger in males and sex differences in splenium area are not reliably present [Bishop andWahlsten, 1997]. More recently CC morphology has been investigated using a variety of neuroimaging methods and measurement parameters, yielding mixed results. For instance, while some investigations comparing adult CC area and the CC/intracranial volume (ICV) ratio between sexes indicate absolute CC area is greater in males, and CC/ICV is greater in females [Smith, 2005; Westerhausen et al., 2011], other work including individuals ranging from 6.7 years old to middle age failed to find sex differences in the CC/ICV ratio [Hasan et al., 2009]. More recently, results of one investigation indicate such differences may be attributed to brain size and not sex differences per se [Bruner et al., 2012], while a subsequent study controlling for age and sex reported larger whole CC area for female subjects [Ardekani et al., 2012].

Questions regarding sex and allometry exist in context of strikingly limited data regarding whole CC morphology and subregion area parameters across a wide age range of the human lifespan. In a cross-sectional sample spanning childhood to late middle age ($N = 99$), subregions projecting to frontal cortical areas reached peak volume at earlier ages than CC subregions that project to the posterior cortex [Hasan et al., 2009]. Pronounced isthmus growth has been reported beginning at age 9 in girls and 11 in boys, suggesting some variation in growth trajectories between sexes in early adolescence [Luders et al., 2010]. It is generally agreed structural CC changes are probably most pronounced in the first 2–3 decades of life, with relatively less structural change through old age [e.g., Hasan et al., 2009; McLaughlin et al., 2007], and only small effects of aging on CC volume were observed over an approximate 1–8-year interval in a cohort of 55 men and 67 women, age 20–85 [Pfefferbaum et al., 2013].

While there have been few comprehensive Magnetic Resonance Imaging (MRI)-based investigations of age-related changes in CC measurement parameters, there have been almost no investigations of CC shape that would permit group comparisons unaffected by size differences. Recently, circularity, the mathematical resemblance of a shape to a circle, has been used to investigate CC morphology [Ardekani et al. 2013]. Circularity is a transformation of area and perimeter sensitive to CC shape change due to myelination, pruning, local or global WM degeneration, or deformation of the CC associated with increasing ventricular volume, among other factors. Because circularity is a composite measure that integrates information relevant to multiple brain-based changes associated with development and aging, it shows promise as a marker of global and local neurological status. In the only prior study to investigate circularity (196 subjects aged 60 or older), values were significantly higher in healthy controls compared to participants with very mild Alzheimer's dementia, and higher in participants with slight versus mild Alzheimer's [Ardekani et al., 2013]. These results were presumably due to CC perimeter deformations and area decreases associated with global brain atrophy and WM degeneration. There are presently no studies to our

knowledge investigating changes in CC circularity from childhood through mid adulthood.

An emphasis on functional correlates of CC morphology has emerged relatively recently [e.g., Fling et al., 2011; Martín-Loeches et al., 2012; Schulte and Müller-Oehring, 2010]. These studies, however, have neither included large numbers of healthy individuals across the lifespan nor used formal mediation analysis to determine whether functional differences are associated with CC development or aging and thus, interpretation of findings has been difficult. It is presently unknown whether the CC allows for more efficient processing due to interhemispheric integration, inhibition of contralateral areas allowing for more efficient lateralized processing, or a combination of both processes in different CC subregions [Schulte and Müller-Oehring, 2010]. Some work suggests that decreasing CC parameters are associated with better neurocognitive performance in children [Ganjavi et al., 2011; Luders et al. 2011; Westerhausen et al., 2011], while positive associations between CC parameters and performance have been reported based on the contrast of older adult and college student samples [Fling et al., 2011].

Because the WM comprising the midsagittal area of the CC offers no morphologically distinct structures to permit reliable segmentation, we used the approach described by Witelson [1989], which is based on non-human primate models and divides the CC into seven subregions, as well as the method proposed by Hampel et al. [1998], which divides the CC into five subregions. Because whole CC and subregion measurement requires reliable identification of the midsagittal plane (MSP), its identification is critical for precise segmentation of the CC to ensure consistency of measurement across individuals. Thus, in this study, we used a highly reliable and previously published segmentation protocol that features automatic identification of the MSP [Ardekani et al., 1997] followed by automated standardization of the magnetic resonance (MR) images along the anterior commissure (AC) and posterior commissure [PC; Ardekani and Bachman, 2009], thus minimizing two sources of operator bias. Subsequently, a recently published automated protocol [Ardekani et al., 2012, 2013] was used to segment the CC based on correspondence to multiple brain atlases, and to generate associated measurement parameters. In this last step, we thus removed a third source of variance associated with CC measurement among individuals.

At present, little is known regarding age-associated changes in MR imaging-based whole CC parameters or CC subregion parameters over the course of the healthy human lifespan. While some prior research has examined sex differences in whole CC area [e.g., Ardekani et al., 2012; Bruner et al., 2012], analyses specific to subregions are limited. Furthermore, the functional importance of any potential sex differences across CC parameters remains unclear. The primary goal of this study was to (1) characterize age associated changes in CC measurement parameters and associated subregions across a wide age range (8–68 years) in a large ($N = 305$) cohort of healthy volunteers while controlling for ICV, (2) assess age $\times$ sex interactions in these CC parameters, and (3) determine the extent to which sex differences mediate neuropsychological functioning.

METHOD

Participants

Three hundred five healthy individuals (52% male) between the ages of 8 and 68 years (mean = 29.50 ± 14.7 years) were recruited through local advertisements and by word of mouth in the community. None of the individuals in this study participated in our prior study [Ardekani et al., 2012]. Written informed consent was obtained from participants or from a parent or guardian if the participant was a minor; all minors provided written assent. Exclusion criteria included any history of a DSM-IV axis I major mood or psychotic disorder as assessed by structured diagnostic interview (Schedule for Affective Disorders and Schizophrenia for School-Age Children—Present and Lifetime Version [Kaufman et al., 1997] or Structured Clinical Interview for DSM-IV disorders Non-Patient Edition [First et al., 2002]). Other exclusion criteria included intellectual or learning disability, MR imaging contraindications, pregnancy, or significant medical illness that could affect the brain. Handedness was determined using the Edinburgh Handedness Inventory [Oldfield, 1971] and mean laterality quotient was 0.74 (standard deviation [SD] = 0.48) and ranged between −1.0 (completely nondextral) to +1.0 (completely dextral).

Image Acquisition

MR imaging exams were conducted at the North Shore University Medical Center on a General Electric 3 Tesla HDx scanner. All scans were reviewed by a radiologist for gross anatomic pathology, which would preclude participation in this study. Scans were also reviewed by a member of the research team and scans with significant artifacts were repeated. Head movement was stabilized with cushions prior to scanning. SPGR images with a 1-mm slice thickness were acquired in the coronal plane (repetition time (TR) = 7.5 ms, echo time (TE) = 3 ms, matrix = 256 $\times$ 256, field of view (FOV) = 240 mm, 216 contiguous images).

Image Processing

The MSP of the CC and regions-of-interest were obtained from raw 3D MR images using the Yuki module within the Automated Registration Toolbox (ART) for CC segmentation [Ardekani, 2013]. Briefly, identification of the MSP was performed for all subjects using a reliable algorithm [Ardekani et al., 1997], which was followed by automated identification of the AC and PC [Ardekani and Bachman, 2009]. Individual

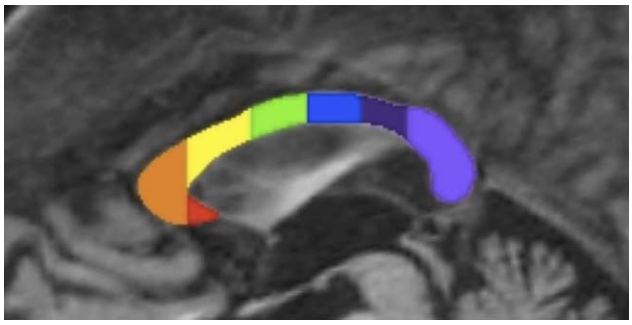

Figure 1.
Witelson Subregion Segmentation. *Notes*. Segmentation using the Witelson [1989] approach was performed automatically by placing five perpendicular lines across the maximum length of the CC at 1/5, 1/3, and 1/2 the distance from the outer limits of the genu and splenium. Subregion 1 (W1, red) corresponds to the rostrum, W2 (orange) corresponds to the genu, W3 (yellow) corresponds to the rostral body, W4 (green) corresponds to the anterior midbody, W5 (blue) corresponds to the posterior midbody, W6 (purple) corresponds to the isthmus, and W7 (lavender) corresponds to the splenium. [Color figure can be viewed in the online issue, which is available at wileyonlinelibrary.com.]

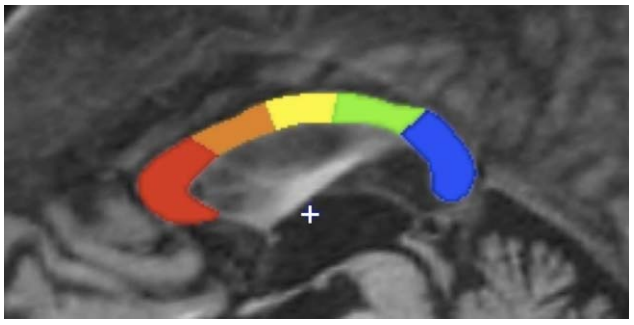

Figure 2.
Hampel Subregion Segmentation. *Notes*. The segmentation scheme proposed by Hampel et al. [1998] was automatically performed by forming a rectangle bordering anterior, posterior, dorsal, and ventral aspects of the CC and projecting 10 rays spaced 36° apart around the center point (+) of the ventral line segment. Four rays within the rectangle constraining the CC divided it into five subregions including C1 (red, genu inclusive of the rostrum), C2 (orange, anterior midbody), C3 (yellow, posterior midbody), C4 (green, isthmus), and C5 (blue, splenium). [Color figure can be viewed in the online issue, which is available at wileyonlinelibrary.com.]

voxels belonging to the CC were identified through automated comparisons between each voxel of the midsagittal slice and 49 brain atlases that were registered to the image based on AC–PC alignment [Ardekani et al., 2012]. All voxels identified as belonging to the CC were labeled as one contiguous structure, extracted and saved in NIFTI image format. The NIFTI image of each midsagittal CC area was visually inspected and manually edited when necessary by an investigator (D. Prendergast) blind to participant characteristics using ITK-Snap [Yushkevich et al., 2006]. The NIFTI images conformed to the CC borders of the original midsagittal MR imaging cross section. Following editing, measurement parameters of the CC were extracted using ART [Ardekani, 2013]. Output data were analyzed using IBM SPSS version 21.0, SAS version 9.2, and SPSS AMOS version 16.

Automated Segmentation and Measurement Parameters

Automated outputs were generated using the Yuki module in ART [Ardekani, 2013], and included area of the midsagittal CC (mm^2), CC perimeter (mm), length (mm), and circularity, as well as the area (mm^2) of seven CC subregions defined by Witelson [1989; Fig. 1], and five CC subregions defined by Hampel et al. [1998; Fig. 2]. The resulting Witelson subregions [Witelson, 1989] included the rostrum (W1), genu (W2), rostral body (W3), anterior midbody (W4), posterior midbody (W5), isthmus (W6), and splenium (W7). Hampel subregions [Hampel et al., 1998] included the genu and rostrum (C1), three midbody sections (C2, C3, C4), and the splenium (C5). Circularity values were calculated as a function of area and perimeter, where circularity is equal to $(4\pi \times \text{area})/\text{perimeter}^2$, with the maximum value of 1 corresponding to a circle and the minimum value of 0 corresponding to a line segment. Intermediate values occur when a less than maximal area is constrained by an object's perimeter.

Intracranial Volume

ICV measurements (mm^3) were generated using the Brainwash module in ART [Ardekani, 2011]. Brainwash is an automated skull-stripping program that identifies which elements of an MR image represent brain tissue (e.g., WM, gray matter, cerebrospinal fluid) based on correspondence to many (>15) MRI atlases of the human brain. Elements of the 3D MRI image other than brain tissue are removed from the MRI image (i.e., skull tissue), and a measurement of the remaining structure yields the ICV.

Neuropsychological Assessments

Subjects were administered 12 neuropsychological tests designed to assess a wide range of functions. Tests were grouped into six domains (processing speed, attention, verbal working memory, spatial working memory, visual learning, and executive functioning) using *z*-score transformations such that higher scores were indicative of better performance. Domains (along with Chronbach's coefficient alpha and sample sizes in parentheses) included: (1) *Speed of Processing* (0.68): Brief Assessment of Cognition in Schizophrenia—Symbol Coding ($n = 240$), Trail Making Test—Part A ($n = 268$); (2) *Attention* (0.85): Continuous Performance Test—identical pairs, average of d′ 2 ($n = 233$), 3 ($n = 232$), and 4 ($n = 232$); (3) *Spatial Working Memory*: Wechsler Memory Scale 3rd edition—spatial span ($n = 240$); (4) *Verbal Functioning* (0.68): Controlled Oral

Word Association Test—total words ($n = 266$), Animal Naming Test ($n = 267$), UMd Letter-Number Span Task ($n = 240$), Hopkins Verbal Learning Test revised—immediate recall, total correct words ($n = 240$); (5) *Visual Learning*: Brief Visuospatial Memory Test revised—total recall ($n = 238$); and (6) *Executive Functioning* (0.69): Neuropsychological Assessment Battery—mazes subtest ($n = 239$), Wisconsin Card Sorting Test—categories completed and percent errors ($n = 152$ and $n = 152$), Trail Making Test—Part B ($n = 268$).

Statistical Analysis

To minimize Type-I error, we examined three-way (age × sex × region) interactions for the Witelson [1989] and Hampel et al. [1998] approaches, respectively, prior to investigating lower-order models. For these analyses, we used a mixed models approach with sex as the between subjects factor and subregion as a within subjects factor with age and age^2 in the model, controlling for ICV. In the Witelson [1989] approach seven subregions included rostrum, genu, rostral body, anterior midbody, posterior midbody, isthmus, and splenium (W1–W7). In the Hampel et al. [1998] approach five subregions included genu/rostrum, three midbody sections, and splenium (C1–C5). In four subsequent analyses, we investigated area, perimeter, length, and circularity with sex as a between subjects factor and age and age^2 in the model, again controlling for ICV. Circularity values were scaled by a factor of 100 to promote model convergence. When interaction terms were significant in quadratic models, linear correlations for each sex were examined before and after peak values as in prior work [Peters et al., 2014]. These analyses were conducted for purely descriptive purposes to characterize age-linked changes independently on each side of peak values, addressing one weakness of quadratic modeling. In all analyses, alpha was set to 0.05 (two-tailed).

When age-by-sex interactions were identified in a given CC region or measurement parameter, path analysis [Kline, 2010] was used to assess whether a given CC parameter meditated the relationship between age and any of the six neuropsychological domains separately for each sex. Path models, which included all six neuropsychological measures, the CC parameter, age and age^2, were considered separately for males and females. We included age^2 in the diagrams to model the nonlinear relationship between age and CC parameter. The relationship between age and neuropsychological measures were determined to be linear (using regression plots); hence no paths were included between age^2 and the neuropsychological measures in the models. An indirect effect was considered significant based on the following two criteria mentioned by Kline [2010, p. 165]. First, Cohen and Cohen's [1983] rule of thumb states that "If all its component unstandardized path coefficients are statistically significant at the same level α, then the whole indirect effect can be taken as statistically significant at the same level α, too." Second, where paths among age, parameter and a neuropsychological domain were all significant, a test recommended by Baron and Kenny [1986], based on the approximate standard error estimates for the indirect effects by Sobel [1986] was used to determine whether significant mediation was present [Kline, 2010; p. 165]. If a and b are unstandardized coefficients for paths $X \rightarrow M$ and $M \rightarrow Y$ then the product ab estimates the unstandardized indirect effect of X on Y through M. If SE_a and SE_b are the corresponding standard errors, then Sobel's estimated standard error of ab is $SE_{ab} = \sqrt{b^2SE_a^2 + a^2SE_b^2}$. In large samples, the ratio $\frac{ab}{SE_{ab}}$ follows approximately a normal distribution and hence a z test (Sobel's test) can be used to reject or accept the null hypothesis that the unstandardized indirect effect is zero.

RESULTS

Male subjects (mean age = 31.5, SD = 15.3) were significantly [$F(1, 303) = 6.37$, $P = 0.012$] older, on average, than female subjects (mean age = 27.3, SD = 13.7). Handedness was not significantly different between male (mean = 0.71, SD = 0.50) and female (mean = 0.78, SD = 0.45) subjects. In addition, there were no significant differences between males (mean = 12.9, SD = 4.0) and females (mean = 12.9, SD = 4.2) in years of education. Descriptive data for all CC measurement parameters is provided in Table I, which includes correlations before and after peak quadratic values for descriptive purposes.

Subregion Analyses

There were significant three-way interactions of age^2 × sex × region for the Witelson [$F(13, 1621) = 5.21$, $P < 0.0001$] and Hampel [$F(9, 1107) = 3.31$, $P = 0.0005$] segmentation approaches, indicating nonuniform differences in subregions between sexes across the age range. In addition, there were significant three-way interactions of age × sex × region for the Witelson [$F(13, 1602) = 6.15$, $P < 0.0001$] and Hampel [$F(9, 1070) = 4.86$, $P < 0.0001$] segmentation approaches. Subsequently, age and age^2 by sex interactions were examined for each individual subregion in both segmentation approaches. Significant interactions of sex × age [$F(1, 299) = 4.11$, $P = 0.043$] and sex × age^2 [$F(1, 299) = 4.20$, $P = 0.041$] were identified in W2 (Fig. 3). Area values for this region peaked at an earlier age for males (32.2 years) than females (40.1 years), with genu area for women surpassing that of men by approximately the fifth decade. A steeper linear slope was observed for females when compared to males prior to the age of the quadratic peak ($r = 0.376$, $P < 0.001$ vs. $r = 0.193$, $P = 0.07$) and females showed a less pronounced linear slope after peak ages were achieved ($r = -0.172$, $P = 0.339$ vs. $r = -0.292$, $P = 0.013$). Nonsignificant interactions between age × sex and age^2 × sex were observed for other

TABLE I. Corpus Callosum Measures

	Mean (SD) values			Age at peak value			Linear slope[a]	
	Sexes combined ($n = 305$)	Men ($n = 160$)	Women ($n = 145$)	Sexes Combined ($n = 305$)	Men (n = 160)	Women ($n = 145$)	Before age peak	After age peak
Area	621.5 (98.9)	637.4 (99.7)	603.9 (95.4)	40.80	38.63	42.31	0.450**	−0.091
Perimeter	203.8 (16.9)	206.3 (17.9)	201.0 (15.3)	51.18	50.31	50.70	0.408**	0.089
Circularity	0.188 (0.023)	0.189 (0.024)	0.187 (0.021)	19.50	8.13	29.82	N/A[b] (m) −0.001 (f)	−0.318** (m) −0.276 (f)
Length	73.7 (5.2)	74.3 (5.4)	73.1 (4.9)	45.02	45.02	44.25	0.410**	0.029
Subregions								
Witelson 1	21.6 (8.8)	22.9 (9.9)	20.3 (7.2)	49.43	48.61	47.59	0.337**	0.193
Witelson 2	137.9 (27.9)	141.4 (30.0)	134.3 (24.8)	35.75	32.19	40.07	0.193 (m) 0.376**(f)	−0.292* (m) −0.172 (f)
Witelson 3	88.5 (16.1)	90.7 (15.8)	86.0 (16.2)	41.88	40.78	43.26	0.324**	−0.017
Witelson 4	72.7 (12.8)	74.7 (12.7)	70.5 (12.7)	40.78	38.63	41.88	0.465**	−0.120
Witelson 5	62.2 (11.4)	63.8 (11.1)	60.5 (11.6)	40.16	38.63	41.62	0.423**	−0.141
Witelson 6	52.7 (12.5)	54.5 (12.0)	50.7 (12.7)	38.63	35.33	40.07	0.257**	−0.110
Witelson 7	185.8 (30.3)	189.5 (31.6)	181.7 (28.4)	45.23	45.02	45.23	0.359**	−0.074
Hampel 1	194.2 (29.9)	198.2 (32.0)	189.7 (26.6)	38.26	36.87	40.07	0.392**	−0.337**
Hampel 2	86.9 (19.3)	89.9 (18.9)	83.5 (19.2)	38.26	35.33	41.88	0.257**	−0.196
Hampel 3	71.2 (16.9)	73.9 (15.6)	68.2 (17.7)	43.26	40.78	45.23	0.288**	−0.045
Hampel 4	75.1 (20.3)	78.9 (18.9)	70.9 (21.0)	45.23	41.35	45.23	0.179**	−0.127
Hampel 5	194.1 (30.4)	196.5 (31.7)	191.5 (28.7)	42.97	42.56	42.91	0.428**	0.007
Intracranial Vol (mm^3)	1,528,168 (182,975)	1,619,129 (160,564)	1,427,796 (151,247)	–	–	–	–	

Note: Univariate statistics are reported for descriptive purposes only.
[a]Slope reported separately for females (f) and males (m) where a significant age by sex interaction was found.
[b]Slope not reported due to an insufficient number of males younger than the peak age.
*Correlation is significant at the 0.05 level (two-tailed); **Correlation is significant at the 0.01 level (two-tailed).

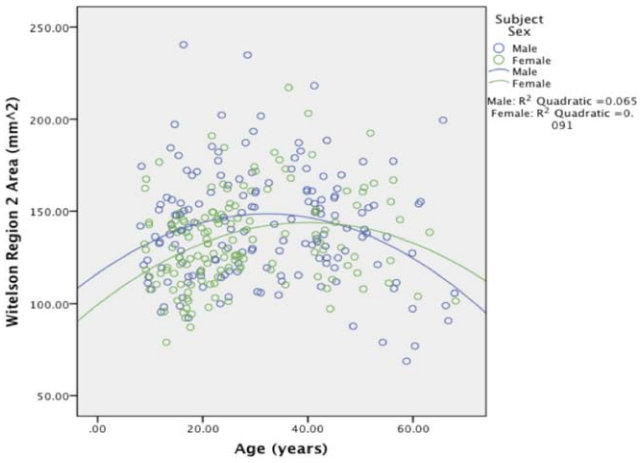

Figure 3.

Witelson Region 2 (W2) Values by Age and Sex. [Color figure can be viewed in the online issue, which is available at wileyonlinelibrary.com.]

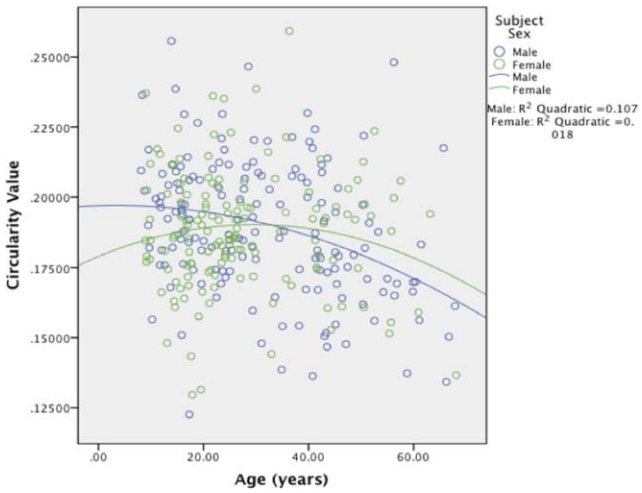

Figure 4.

Circularity Values by Age and Sex. [Color figure can be viewed in the online issue, which is available at wileyonlinelibrary.com.]

Witelson subregions and all Hampel subregions. Two-way interactions (age × sex and age^2 × sex) were not statistically significant using either the Witelson or Hampel approaches (P's > 0.05). There were no significant main effects of sex using either approach (P's > 0.05). The main effect of age^2 was significant for both the Witelson and Hampel approaches [$F(1, 299) = 22.83$, $P < 0.0001$].

Whole CC Parameter Analyses

We examined age × sex and age^2 × sex interactions for the four additional CC measurement parameters. Neither significant age × sex nor age^2 × sex interactions were identified for area, perimeter, or length measurements (P's > 0.05). However, significant age × sex [$F(1, 299) = 4.83$, $P = 0.029$] and age^2 × sex [$F(1, 299) = 4.20$, $P = 0.041$] interactions were observed for CC circularity. Peak circularity values were observed at the low end of the age range for males (8.13 years), while circularity values for females peaked in the third decade (29.8 years) as illustrated in Figure 4. A more pronounced negative linear slope was observed in males ($r = -0.318$, $P < 0.001$) compared to females ($r = -0.276$, $P = 0.069$) following quadratic age peaks. Male circularity values were lower than female values after the mid-30s. Main effects of age and age^2 were not significant predictors of circularity (P's > 0.070), though main effects of sex were found when predicting CC circularity in models including linear [$F(1, 299) = 7.63$, $P = 0.006$] and quadratic [$F(1, 299) = 7.00$, $P = 0.009$] age terms. Significant main effects of age and age^2 for analyses investigating area, perimeter, and length (all $P < 0.001$) indicate that values for these three parameters increased with age, with peak values observed in the early to mid 40s. Using the age^2 term significant main effects were identified for sex when predicting perimeter [$F(1, 299) = 4.25$, $P = 0.040$] and length [$F(1, 299) = 4.15$, $P = 0.042$], indicating that these measures were larger in males even while controlling for ICV.

Mediation Analysis

Four path diagrams (two per sex) were constructed to assess whether W2 or circularity mediated the relationship between age (including age and age^2 terms) and any of the six neuropsychological domains. W2 significantly mediated different neuropsychological domains for male and female subjects. Path diagrams including significant maximum likelihood estimates for male and female subjects can be found in Figures 5 and 6. Specifically, for females, W2 area significantly mediated the relationship between age and (relatively stable) performance on processing speed tasks across the observed age range ($z = 4.87$, $P < 0.001$). For male participants, W2 area significantly mediated the relationships between age and visual learning ($z = -1.99$, $P = 0.048$), and age and executive functioning ($z = -2.95$, $P = 0.015$). In contrast to processing speed, both visual learning and executive functioning were characterized by linear decreases across the age range. CC shape as indexed by circularity did not significantly mediate any domain of neuropsychological functioning for either sex (all P's > 0.05).

DISCUSSION

To our knowledge, this is the largest MR imaging study to investigate the effects of age and sex on multiple indices of CC morphology in healthy individuals, and the first to feature contrasting segmentation approaches. Overall, our findings suggest CC area, perimeter, length, and circularity are characterized by inverted U-shaped curves across the lifespan with evidence for sex differences in genu size and

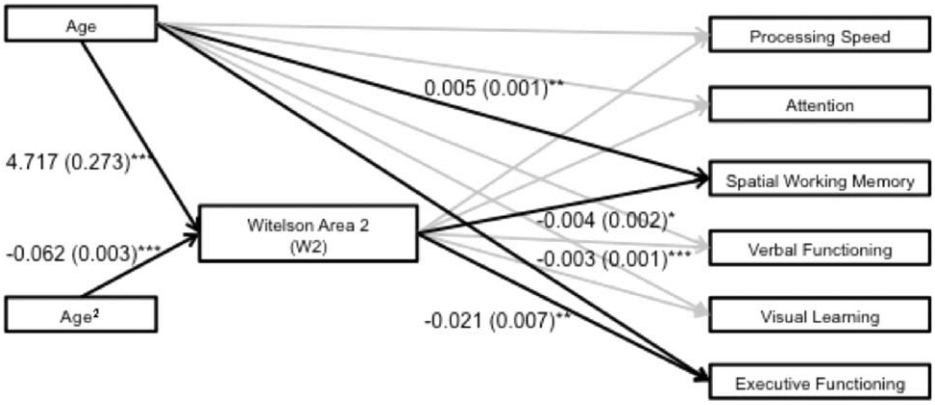

Figure 5.

Path diagram reflecting significant maximum likelihood estimates (standard errors) for male subjects. Significance level of maximum likelihood estimates: *≤0.05, **≤0.01, ***≤0.001. Black lines reflect significant maximum likelihood estimates ($P \leq 0.05$), gray lines reflect nonsignificant findings ($P > 0.05$). [Color figure can be viewed in the online issue, which is available at wileyonlinelibrary.com.]

circularity. We also observed changes in genu morphology have differential functional significance in males and females. Important methodologic strengths of our study include the use of reliable and automated algorithms for identification of the MSP [Ardekani et al., 1997], AC and PCs [Ardekani and Bachman, 2009] and atlas-based segmentation of the CC [Ardekani et al. 2012a, b], thus minimizing three sources of operator bias. In this regard, potentially important limitations of prior studies examining the CC is the lack of standardization of the brain along the AC and PCs in the MSP and/or manual tracing of the CC [e.g., Dubb et al., 2003; Hasan et al., 2009; Lebel et al., 2010; Suganthy et al., 2003; Westerhausen et al., 2011]. In addition, prior studies investigating sex differences also focused on an age range restricted to children or adults [e.g., Bruner et al., 2012; Dubb et al., 2003; Giedd et al., 1997; Luders et al., 2010] or a smaller number of participants [e.g., Hasan et al., 2009; Holloway and DeLacoste, 1986; McLaughlin et al., 2007; Pfefferbaum et al., 2013]. Moreover, few MR imaging investigations have used nonlinear modeling [e.g., Pfefferbaum et al., 2013] across the lifespan while investigating these measures in relationship to neuropsychological functioning.

In this study, main effects for sex controlling for ICV were found when predicting CC length, perimeter, and circularity, but neither whole CC area nor any of its

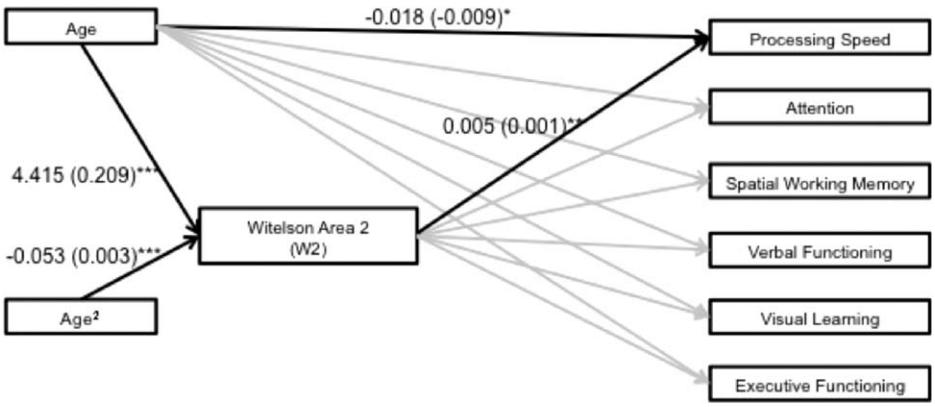

Figure 6.

Path diagram reflecting significant maximum likelihood estimates (standard errors) for female subjects. Significance level of maximum likelihood estimates: *≤0.05, **≤0.01, ***≤0.001. Black lines reflect significant maximum likelihood estimates ($P \leq 0.05$), gray lines reflect nonsignificant findings ($P > 0.05$). [Color figure can be viewed in the online issue, which is available at wileyonlinelibrary.com.]

subregions. In this study, male callosa were longer than females with greater perimeter while controlling for ICV. In a relatively large ($N = 102$), study featuring young adults aged 18–27, Bruner et al. [2012] reported that differences in midsagittal CC size and shape between males and females were primarily associated with brain size and not sex per se. Luders et al. [2014] reported similar findings in an investigation of callosal thickness using a small number of male and female participants matched for brain size. Previously, a meta-analysis including 41 studies from 1982 to 1994, five of which reported significant sex-related size differences, found that sex differences accounted for roughly 1% of variance in CC size between sexes [Bishop and Wahlstein, 1997]. More recently several studies have failed to identify significant CC sex differences [e.g., Fling et al., 2011; Hasan et al., 2009; Westerhausen et al., 2011]. In contrast, however, Ardekani et al. [2012], found whole CC area was significantly larger in female subjects when statistically controlling for age and ICV in a linear model, and also when matching a subsample of male and female participants by total brain size. Differences between our study and Ardekani et al. [2012] may be related to our inclusion of 88 subjects between 8 and 17 years of age and their inclusion of 73 subjects ages 70–94.

Our findings indicate that across all subjects the genu and isthmus reached peak area values earliest, followed by the body, the splenium and finally the rostrum. Moreover, genu area segmented using the Witelson approach reached peak values earlier in males compared to females, with significant linear slopes observed prior to the peak age in females and after the peak age in males. The large difference in peak ages between the genu and rostrum lends support to Witelson's [1987] decision to separate these two regions and contrasts with the approach used by Hampel et al. [1998] wherein these subregions are combined. It is noteworthy, however, that with both approaches males reached peak area values before females, most prominently in the genu. A similar pattern of pronounced growth in childhood, slight volume decline in adulthood, and later peak area values (early 30's) was reported by Hasan et al. [2009], although this work featured CC volumes derived from diffusion tensor imaging (DTI) fiber tracking. To our knowledge, no prior studies investigated linear slopes on either side of quadratic peak ages. Peak whole CC area (40.8 years), indicated ongoing myelination until early middle age, with a significant positive linear relationship observed before the peak value. A nonsignificant negative slope observed after the peak is partially consistent with Pfefferbaum et al. [2013] who reported nonsignificant changes in CC volume after age 20 in both sexes. In contrast to Pfefferbaum et al. [2013], however, our results suggest that CC growth continues until early middle age.

We identified sex differences across the age range localized to W2 using the Witelson approach. Genu area segmented using the Witelson [1989] approach appears to reach peak values earlier in males (32.2 years) than in females (40.1 years), with significant linear slopes observed prior to peak age in females and after peak age in males. Greater absolute area values were observed in males until the fifth decade. This finding was not observed in C1 (comprising the genu and rostrum) in the Hampel approach. Significant sex differences across the lifespan in genu area in this study may be due to differences in the number of interhemispheric fibers between males and females at different stages of life, as the density of myelinated and unmyelinated fibers in the CC does not appear to vary with sex or CC area [Aboitiz et al., 1992]. When creating her segmentation scheme, Witelson [1989] judged the rostrum to be separate from the genu, based on primate models, human dissection studies, and radiographic tracer studies. This differentiation is supported by work featuring tractography, which reports that the main body of the genu projects primarily to the anterior frontal cortex, while the rostrum projects primarily to orbitofrontal cortex [Lebel et al., 2010]. Compared to the body of the CC, the genu is composed predominantly of smaller (0.2–1.0 μm) fibers and substantially more unmyelinated fibers [Aboitiz et al., 1992].

The finding that age × sex and age^2 × sex interactions significantly predicted CC circularity indicates its shape changes differently between sexes across the lifespan. Previous reports of CC shape differences between sexes exist, although methods and measurement parameters have not been comparable among studies. For example, some studies used template deformation morphometry or surface based mesh modeling to yield CC thickness or bending angle [e.g., Dubb et al., 2003; Narr et al., 2000; Walterfang et al., 2009]. This study is the first to utilize the parameter of circularity across a wide age range of healthy volunteers that includes both children and adolescents. In males, circularity values peaked near the minimum of the observed age range and assumed a significant negative trajectory through old age. For female participants, a parabolic trajectory was observed with the peak value observed at age 29.8 and nonsignificant linear trends on both sides of the peak age. While significant interactions were not found for CC area, perimeter, and length values between sexes across the observed age range, shape changes indexed by circularity were pronounced in men.

To our knowledge, this is the largest study to examine circularity across the lifespan and thus, the inclusion of this parameter allows for a conceptually coherent description of significant sex differences in CC shape. As a shape measure, circularity is invariant to object size, demonstrated by the lack of significant correlations between circularity and ICV and no differences in the circularity × age × sex interaction while controlling versus not controlling for ICV. Because circularity is a transformation of area and perimeter, it can be perfectly predicted when these parameters are known, and it is reasonable to question whether measuring circularity adds substantial information to area and perimeter. In our data, circularity appears to offer a unique view of CC development between sexes, as age × sex and age^2 × sex interactions were

present when predicting circularity, but not area, perimeter, or length (controlling for ICV). Because circularity has conceptual meaning as a shape measure, it is far more comprehensible than other arbitrary transformations of area and perimeter that could potentially detect such interactions.

Numerous studies have investigated the functional correlates of CC morphology in healthy volunteers. Decreased area in the genu (W2 specifically) has been associated with poorer working memory and psychomotor performance in older (over 65), but not young adult samples [Fling et al., 2011]. Diffusion properties in the genu have been associated with working memory, processing speed, and executive functioning, but not episodic memory [Kennedy and Raz, 2009]. Age-related decline in splenium diffusion properties predicted memory and executive functioning [Voineskos et al., 2012]. The genu has been implicated in interhemispheric inhibition as opposed to interhemispheric integration, which was associated with the posterior CC [Schulte and Muller-Oehring, 2010]. With respect to shape, one recent study in young adults (ages 18–27) reported better performance on attention and response inhibition tasks associated with thinner and more curved CC [Martín-Loeches et al., 2012].

Of the two CC parameters that demonstrated sex differences, only W2 emerged as a mediator of neuropsychological functioning. For males, the pattern of development and aging that characterized W2 mediated linear decreases with age for both executive and visual learning performance. In contrast, for females the age-linked trajectory of W2 area mediated the relationship between age and processing speed. In contrast to executive functioning and visual learning performance, processing speed values did not vary with age. To date, no known investigation of cross-sectional CC measurement parameters has featured such a mediation analysis across this range of the lifespan in healthy controls. Fling et al. [2011] reported a positive correlation between W2 and W4 and a cognitive composite composed of verbal working memory and processing speed that was present in an older (65–80), but not a younger group (18–30). Other work indicates that the CC is related to global intellectual functioning (IQ). For example, Luders et al. [2007] reported that posterior CC thickness is positively correlated with IQ in adults, while others report significant negative associations between callosal thickness and IQ in children, primarily driven by males [Ganjavi et al., 2011; Luders et al., 2011]. In addition, in one sample of young adults increasing attentional control was associated with CC thinness and curvature using procrustes analysis [Bruner et al., 2012].

This work has several limitations that should be acknowledged. With the increasing use of diffusion tensor imaging other CC segmentation approaches have been reported based on connectivity between midsagittal CC and cortical regions of interest [Hasan et al., 2009; Huang et al., 2005; Lebelet al., 2010], as well as Brodmann areas [Chao et al., 2009]. Investigation of the effects of age and sex in relationship to CC morphology was restricted to gross anatomy and some work suggests that diffusion tensor imaging may be a more sensitive technique for assessing WM properties [Fjell et al., 2009]. It should be acknowledged, however, that structural morphology and diffusion tensor imaging [Voineskos et al., 2012] can provide complementary information and may not directly correlate with one another [Tamnes et al., 2011]. For example, in this study, whole CC and subregion areas peaked later when compared to diffusion tensor imaging studies, which reported peak diffusion properties in the early 20's in anterior regions and peak values in posterior regions as late as the early 30's [Hasan et al., 2009, Lebel et al. 2010]. This suggests that 2D parcellation schemes remain informative and valuable, and multiple authors suggest conducting 2D segmentation following fiber tracking using novel parcellation schemes [e.g., Chao, 2009; Hofer and Frahm, 2006]. It should be noted, however, that some DTI-based CC segmentation algorithms [e.g., Hofer and Frahm, 2006] may not present a compelling alternative to Witelson's [1989] parcellation scheme, which is not surprising given that Witelson's work was developed based on dissection studies. At the present time, there is no well-established DTI-based parcellation scheme for CC segmentation, but rather a common focus on large cortical regions of interest (ROIs) that differ among studies, which are used for this purpose. Given that Witelson's parcellation scheme is well-established, easily implemented in a large number of subjects, and tracks well with results from dissection and DTI work, it remains the most practical parcellation scheme for the present purposes.

An additional limitation stems from the reduction of data secondary to the limited number of subregions included in the Witelson [1989] and Hampel et al. [1998] parcellation schemes. To this point, it may also be argued that DTI-based segmentations that feature 5–7 large cortical ROIs still represent coarse parcellation. An exception is the study by Chao et al. [2009] who used 28 Brodmann areas to characterize connectivity between midsagittal CC and cortex. Other methods for characterizing the CC using MRI [e.g., Luders et al., 2010] offer more measurement points (e.g., more thickness values), and consequently more detailed data sensitive to local change. In this study, fewer measurements facilitated mediation analysis. Lastly, although both segmentation schemes have been widely used in the literature, they may still represent somewhat arbitrary subdivisions regarding the underlying neuroanatomy; however, it should be noted that the reliability of these metrics is much higher compared to other imaging modalities, including diffusion tensor imaging, which can be noisier.

In sum, we demonstrate sex differences across the lifespan in the human CC that were localized to the genu, and associated with neuropsychological functioning. Negative findings observed in CC regions other than W2 while controlling for ICV suggest that previous reports of sex differences outside of the genu may be due to allometric factors. Taken together, this study allows for a clearer understanding of various CC parameters across the

lifespan in healthy humans, and may have implications for future investigations of atypical development in psychiatric disorders [e.g., Bearden et al., 2011]. Moreover, CC structural alterations may be suitable for use as endophenotypes for genetic mapping of psychiatric disorders based on heritability studies [Fears et al. 2014].

REFERENCES

Aboitiz F, Scheibel AB, Fisher RS, Zaidel E (1992): Fiber composition of the human corpus callosum. Brain Res 598:143–153.

Ardekani BA (2011): Brainwash module of the Automatic Registration Toolbox (ART). Available at: http://www.nitrc.org/projects/art. Last Accessed May 1, 2014

Ardekani BA (2013): Yuki module of the Automatic Registration Toolbox (ART) for corpus callosum segmentation. Available at: http://www.nitrc.org/projects/art. Last Accessed May 1, 2014

Ardekani BA, Kershaw J, Braun M, Kanno I (1997): Automatic detection of the mid-sagittal plane in 3-D brain images. IEEE Trans Med Imaging 16:947–952.

Ardekani BA, Figarsky K, Sidtis JJ (2012): Sexual dimorphism in the human corpus callosum: An MRI study using the OASIS brain database. Cereb Cortex 23:2514–2520.

Ardekani BA, Bachman AH, Figarsky K, Sidtis JJ (2013): Corpus callosum shape changes in early Alzheimer's disease: An MRI study using the OASIS brain database. Brain Struct Funct 219: 1–10.

Baron RM, Kenny DA (1986): The moderator-mediator variable distinction in social psychological research: Conceptual, strategic and statistical considerations. J Pers Soc Psychol 51:1173–1182.

Bearden CE, van Erp TG, Dutton RA, Boyle C, Madsen S, Luders E, Kieseppa T, Tuulio-Henriksson A, Huttunen M, Partonen T, Kaprio J, Lönnqvist J, Thompson PM, Cannon TD (2011): Mapping corpus callosum morphology in twin pairs discordant for bipolar disorder. Cereb Cortex. 2011;21:2415–2424.

Bishop KM, Wahlsten D (1997): Sex differences in the human corpus callosum: Myth or reality? Neurosci Biobehav Rev 21:581–601.

Bruner E, de la Cuétara JM, Colom R, Martin Loeches M (2012): Gender based differences in the shape of the human corpus callosum are associated with allometric variations. J Anat 220: 417–421.

Chao YP, Cho KH, Yeh CH, Chou KH, Chen JH, Lin CP (2009): Probabilistic topography of human corpus callosum using cytoarchitectural parcellation and high angular resolution diffusion imaging tractography. Hum Brain Mapp 30:3172–3187.

DeLacoste-Utamsing C, Holloway RL (1982): Sexual dimorphism in the human corpus callosum. Science 216:1431–1432.

Dubb A, Gur R, Avants B, Gee J (2003): Characterization of sexual dimorphism in the human corpus callosum. Neuroimage 20: 512–519.

Fears SC, Service SK, Kremeyer B, Araya C, Araya X, Bejarano J, Ramirez M, Castrillón G, Gomez-Franco J, Lopez MC, Montoya G, Montoya P, Aldana I, Teshiba TM, Abaryan Z, Al-Sharif NB, Ericson M, Jalbrzikowski M, Luykx JJ, Navarro L, Tishler TA, Altshuler L, Bartzokis G, Escobar J, Glahn DC, Ospina-Duque J, Risch N, Ruiz-Linares A, Thompson PM, Cantor RM, Lopez-Jaramillo C, Macaya G, Molina J, Reus VI, Sabatti C, Freimer NB, Bearden CE (2014): Multisystem component phenotypes of bipolar disorder for genetic investigations of extended pedigrees. JAMA Psychiatry. 2014;71:375–387.

First MB, Spitzer RL, Gibbon M, Williams JBW (2002): Structured Clinical Interview for DSM-IV-TR Axis I Disorders, Research Version, Non-patient Edition. (SCID-I/NP). New York: Biometrics Research, New York State Psychiatric Institute.

Fjell AM, Westlye LT, Amlien I, Espeseth T, Reinvang I, Raz N, Agartz I, Salat DH, Greve DN, Fischl B, Dale AM, Walhovd KB 2009. High consistency of regional cortical thinning in aging across multiple samples. Cerebral Cortex 19:2001–2012.

Fling BW, Chapekis M, Reuter-Lorenz PA, Anguera J, Bo J, Langan J, Welsh RC, Seidler RD (2011): Age differences in callosal contributions to cognitive processes. Neuropsychologia 49:2564–2569.

Ganjavi H, Lewis JD, Bellec P, MacDonald PA, Waber DP, Evans AC, Karama S (2011): Negative associations between corpus callosum midsagittal area and IQ in a representative sample of healthy children and adolescents. PloSOne 6:e19698.

Giedd JN, Castellanos FX, Rajapakse JC, Vaituzis AC, Rapoport JL (1997): Sexual dimorphism of the developing human brain. Prog Neuropsychopharmacol Biol Psychiatry 21:1185–1201.

Hampel H, Teipel SJ, Alexander GE, Horwitz B, Teichberg D, Schapiro MB, Rapoport SI (1998): Corpus callosum atrophy is a possible indicator of region-and cell type-specific neuronal degeneration in Alzheimer disease: A magnetic resonance imaging analysis. Arch Neurol 55:193–198.

Hasan KM, Kamali A, Kramer LA, Papnicolaou AC, Fletcher JM, Ewing-Cobbs L (2009): Diffusion tensor quantification of the human midsagittal corpus callosum subdivisions across the lifespan. Brain Res 1227:52–67.

Hofer S, Frahm J (2006): Topography of the human corpus callosum revisited—Comprehensive fiber tractography using diffusion tensor magnetic resonance imaging. Neuroimage 32: 989–994.

Holloway RL, DeLacoste MC (1986): Sexual dimorphism in the human corpus callosum: An extension and replication study. Hum Neurobiol 5:87–91.

Huang H, Zhang J, Jiang H, Wakana S, Poetscher L, Miller MI, van Zijl PCM, Hillis AE, Wytik, R, Mori S (2005): DTI tractography based parcellation of white matter: Application to the mid-sagittal morphology of corpus callosum. Neuroimage 26: 195–205.

Kaufman J, Birmaher B, Brent D, Rao UMA, Flynn C, Moreci P, Williamson D Ryan N (1997): Schedule for affective disorders and schizophrenia for school-age children-present and lifetime version (K-SADS-PL): Initial reliability and validity data. J Am Acad Child Adolesc Psychiatry 36:980–988.

Kennedy KM, Raz N (2009): Aging white matter and cognition: Differential effects of regional variations in diffusion properties on memory, executive functions, and speed. Neuropsychologia 47:916–927.

Kline RB (2010): Principles and Practice of Structural Equation Modeling. New York: Guilford press.

Lebel C, Caverhill-Godkewitsch S, Beaulieu C (2010): Age-related regional variations of the corpus callosum identified by diffusion tensor tractography. Neuroimage 52:20–31.

Luders E, Narr KL, Bilder RM, Thompson PM, Szeszko PR, Hamilton L, Toga AW (2007): Positive correlations between corpus callosum thickness and intelligence. Neuroimage 37: 1457–1464.

Luders E, Thompson PM, Toga AW (2010): The development of the corpus callosum in the healthy human brain. J Neurosci 30:10985–10990.

Luders E, Thompson PM, Narr KL, Zamanyan A, Chou YY, Gutman B, Toga AW (2011): The link between callosal thickness and intelligence in healthy children and adolescents. Neuroimage 54:1823–1830.

Luders E, Toga AW, Thompson PM (2014): Why size matters: Differences in brain volume account for apparent sex differences in callosal anatomy. Neuroimage 84:820–824.

Martín-Loeches M, Bruner E, de la Cuétara JM, Colom R (2012): Correlation between corpus callosum shape and cognitive performance in healthy young adults. Brain Struct Funct 218: 721–731.

McLaughlin NC, Paul RH, Grieve SM, Williams LM, Laidlaw D, DiCarlo M, Clark CR, Whelihan W, Cohen RA, Whitfor TJ, Gordon E (2007): Diffusion tensor imaging of the corpus callosum: A cross-sectional study across the lifespan. Int J Dev Neurosci 25:215–221.

Narr KL, Thompson PM, Sharma T, Moussai J, Cannestra AF, Toga AW (2000): Mapping morphology of the corpus callosum in schizophrenia. Cereb Cortex 10:40–49.

Oldfield RC (1971): The assessment and analysis of handedness: The Edinburgh inventory. Neuropsychologia 9:97–113.

Peters BD, Ikuta T, DeRosse P, John M, Burdick KE, Prendergast D, Szeszko PR, Malhotra AK (2014): Age-related differences in white matter tract microstructure are associated with cognitive performance from childhood to adulthood. Biol Psychiatry 75: 248–256.

Pfefferbaum A, Rohlfing T, Rosenbloom MJ, Chu W, Colrain IM, Sullivan EV (2013): Variation in longitudinal trajectories of regional brain volumes of healthy men and women (ages 10 to 85 years) measures with atlas-based parcellation of MRI. Neuroimage 65:176–193.

Schulte T, Müller-Oehring EM (2010): Contribution of callosal connections to the interhemispheric integration of visuomotor and cognitive processes. Neuropsychol Rev 20:174–190.

Smith R (2005): Relative size versus controlling for size. Curr Anthropol 46:249–273.

Suganthy J, Raghuram L, Antonisamy B, Vettivel S, Madhavi C, Koshi R (2003): Gender-and age-related differences in the morphology of the corpus callosum. Clin Anat 16:396–403.

Tamnes CK, Fjell AM, Østby Y, Westlye LT, Due-Tønnessen P, Bjørnerud A, Walhovd KB (2011): The brain dynamics of intellectual development: Waxing and waning white and gray matter. Neuropsychologia 49:3605–3611.

van der Knaap LJ, van der Ham IJ (2011): How does the corpus callosum mediate interhemispheric transfer? A review. Behav Brain Res 223:211–221.

Voineskos AN, Rajji TK, Lobaugh NJ, Miranda D, Shenton ME, Kennedy JL, Pollock BG, Mulsant BH (2012): Age-related decline in white matter tract integrity and cognitive performance: A DTI tractography and structural equation modeling study. Neurobiol Aging 33:21–34.

Walterfang M, Wood AG, Reutens DC, Wood SJ, Chen J, Velakoulis D, McGorry PD,Pantelis C (2009): Corpus callosum size and shape in first-episode affective and schizophrenia-spectrum psychosis. Psychiatry Res Neuroimaging 173:77–82.

Westerhausen R, Kompus K, Dramsdahl M, Falkenberg LE, Grüner R, Hjelmervik H, Specht K, Plessen K, Hugdahl K (2011): A critical re-examination of sexual dimorphism in the corpus callosum microstructure. Neuroimage 56:874–880.

Witelson S (1989): Hand and sex differences in the isthmus and genu of the human corpus callosum: A postmortem morphological study. Brain 112:799–835.

Yushkevich PA, Piven J, Hazlett HC, Smith RG, Ho S, Gee JC, Gerig G (2006): User-guided 3D active contour segmentation of anatomical structures: Significantly improved efficiency and reliability. Neuroimage 31:1116–1128.